We are IntechOpen,
the world's leading publisher of
Open Access books
Built by scientists, for scientists

4,800

Open access books available

122,000

International authors and editors

135M

Downloads

Our authors are among the

154

Countries delivered to

TOP 1%

most cited scientists

12.2%

Contributors from top 500 universities

CLARIVATE ANALYTICS

BOOK CITATION INDEX

INDEXED

WEB OF SCIENCE™

Selection of our books indexed in the Book Citation Index
in Web of Science™ Core Collection (BKCI)

Interested in publishing with us?
Contact book.department@intechopen.com

Numbers displayed above are based on latest data collected.
For more information visit www.intechopen.com

Inhomogeneous Material Modelling and Characterization for Aluminium Alloys and Welded Joints

Jisen QIAO and Wenyan WANG

College of Materials Science and Engineering, Lanzhou University of Technology
P.R China

1. Introduction

Structure functions are decided by the material properties which made of it. Material modelling and characterization are important to crashworthiness of automobile. Some times right material parameters are the key to the models which describe large deformation and failure behaviours of car body. Therefore aimed at the dynamic behaviours of aluminium alloy in certain crashing state with high strain rate, triaxiality, and damage initialization etc., large work has been done in this field including component and full scare crashing tests, which cost a lot. However, the result is not satisfied. Detail information about the crashing is hard to obtained from the experiments because of the high rate and limited time of deformation (in some specific cases, the strain rate is over 2×10^2). Simulation is an effective method to extend the experimental data for complete models of crashworthiness.

In certain degree, the precision of simulation is depended on the authority of material parameters of modelling. Large deformation during crashing is an complicated process including various stages of elastic deformation, plastic deformation, damage initialization, evolution and failure. Strain rate, anisotropy and stress state make effects on this process. How do these factors exactly work? Still so many questions are left in this field. Smooth tension tests combined with simulation were carried out for material modelling and characterization of aluminium alloy AW 6061 (Blauel & Su, 2002; Sun, 2003). Static and dynamic response of typical aluminium alloy components is predicted successfully by using G-T-N damage mode for FEM simulation. The damage model explains the ductile fracture of the aluminium and its initiation and evolution by mechanism of growth of voids that could be applied in industry. Dynamical loading was established by using explicit solver of FEM code (Franck & Bruno, 2001). This model takes elastic flow and anisotropic into account. Thereby this could be used to predict situation of damage and fracture of materials with obvious texture deformation such as extruded aluminium alloys in circumstances of dynamic loading with large deformation. Another contribution of Frank's research is to develop iterative algorithm which has an experiment combined with numerical simulation to achieve optimizing parameters in material characterization. This algorithm uses data from notch tensile as the basic input to derive parameters of G-T-N damage model, and revise these parameters by FEM calculation in consider of anisotropic influence. Eventually, the result of numerical simulation fit with experiments. In comparing with other method of

material characterization, this could avoid a great amount of experiment expenses, and improving the efficiency of modelling.

Meanwhile, the inhomogeneous deformation and failure of welded joints and components have become a key problem for crashworthiness of light automobile. There is much dissimilarity in mechanical behaviour between welded and un-welded metal, evaluation of the mechanical properties of welded joint has become a hot topic in the research world. Material modelling and characterization for aluminium alloy welded joints are focused in this chapter.

Joint strength was evaluated as a function of strength mismatch factors and the geometric size of HAZ (Zhu et al., 2004). The author used FEM analysis of tensile specimens in comparison with test results to study the stress distribution in tension plate samples. Finally, Zhu identified an analytical approach to predict tensile strength of mismatch joints for pipeline steel. Asif Husain, Sehgal D k, et al. Another inverse finite element procedure was developed by carrying out with the commercial FE code, such as ABAQUS to determine constitutive tensile behaviour of homogeneous materials (Asif et al., 2004). More experimental research results have been reported by other scholars (Campitelli et al., 2004; Hankin et al, 1998). A series of analytical equations based on a force-distribution assumption were formulated to describe mechanical properties of a tailor blank welded by a CO_2 laser (B.Y. Ghoo et al., 2001). Actually, the results demonstrate the average mechanical property of welds and HAZ, which can not precisely describe the effect of micro zone on the general mechanical behaviour of a joint. It is necessary to develop experimental techniques and analytical methods in order to quantitatively evaluate the material mechanical heterogeneity.

In this chapter, an inverse finite element procedure is developed and executed using the ABAQUS computer code for the determination of the constitutive tensile behavior of welded metals. The proposed inverse technique is based on the small punch shearing law. The validation of numerical modeling is identified compared with uniaxial tensile tests.

2. Material modelling and characterization for basic aluminium alloy under static and dynamic loading

2.1 Experiment procedure
2.1.1 General idea
Alminium alloy 5052H34 and 6063T6 are widely used for welded structure of car body because of their remarkable performance in welding as well as forming process. In actual collision, these structures would mostly have large plastic deformation before failure. Therefore, it's not enough for material characterization only testing yield and ultimate strength, more work should be done in work hardening, anisotropic and facture features of initiated damage. As for specific aluminium alloy, the welded structure is fixed, however the work temperature and loading condition varies with the actual impact process. In accordance with the actual impact condition, various tensile tests under static and dynamic loading are carried out for aluminium alloy. The experiments were divided into five groups, which are smooth tensile, notch tensile, double notch tensile, Iosipescu shear test, and dynamic tensile test. Serial number of the test specimens and experiment condition are show in Table.1, sizes of the specimens are show in Fig.1, the specimens are cut from original plate, the distribution of all the specimens on plate can be seen on Fig 2.

Test Style	Cross section (mm²)	Gauge Length (mm)	Sample No.	Load Speed (mm/s)	Strain Rate s⁻¹
Smooth Tensile	2.897×5.037	10	PT1-UT-S1Q	0.01	Static
	2.894×5.042	10	PT1-UT-S2Q	0.01	Static
	2.889×5.029	10	PT1-UT-S3Q	0.01	Static
	2.889×5.029	10	PT1-UT-S1L	0.01	Static
	2.885×5.025	10	PT1-UT-S2L	0.01	Static
	2.893×5.031	10	PT1-UT-S3L	0.01	Static
Notch Tensile	2.889×5.025	10	PT1-UNT-S1Q	0.01	Static
	2.892×5.033	10	PT1-UNT-S2Q	0.01	Static
	2.889×5.030	10	PT1-UNT-S3Q	0.01	Static
Double Notch Tensile	2.787×5.123	10	PT1-DNT-S1Q	0.01	Static
	2.789×5.132	10	PT1-DNT-S2Q	0.01	Static
	2.785×5.134	10	PT1-DNT-S3Q	0.01	Static
	2.788×5.128	10	PT1-DNT-S1L	0.01	Static
	2.787×5.133	10	PT1-DNT-S2L	0.01	Static
	2.791×5.128	10	PT1-DNT-S3L	0.01	Static
Iosipescu Shear Test	2.796×4.029	10	PT1-PSC-S1L	0.01	Static
	2.792×4.031	10	PT1-PSC-S2L	0.01	Static
	2.795×4.034	10	PT1-PSC-S3L	0.01	Static
	2.794×4.033	10	PT1-PSC-S1Q	0.01	Static
	2.793×4.032	10	PT1-PSC-S2Q	0.01	Static
	2.792×4.034	10	PT1-PSC-S3Q	0.01	Static
Dynamic Tensile	2.892×5.038	10	PT1-UT-D1Q	$1.7×10^3$	143
	2.888×5.036	10	PT1-UT-D2Q	$1.7×10^3$	143
	2.883×4.997	10	PT1-UT-D3Q	$1.7×10^3$	143
	2.892×5.035	10	PT1-UT-D4Q	$1.7×10^3$	143
	2.888×5.033	10	PT1-UT-D5Q	$1.7×10^3$	143
	2.883×4.995	10	PT1-UT-D6Q	$1.7×10^3$	143

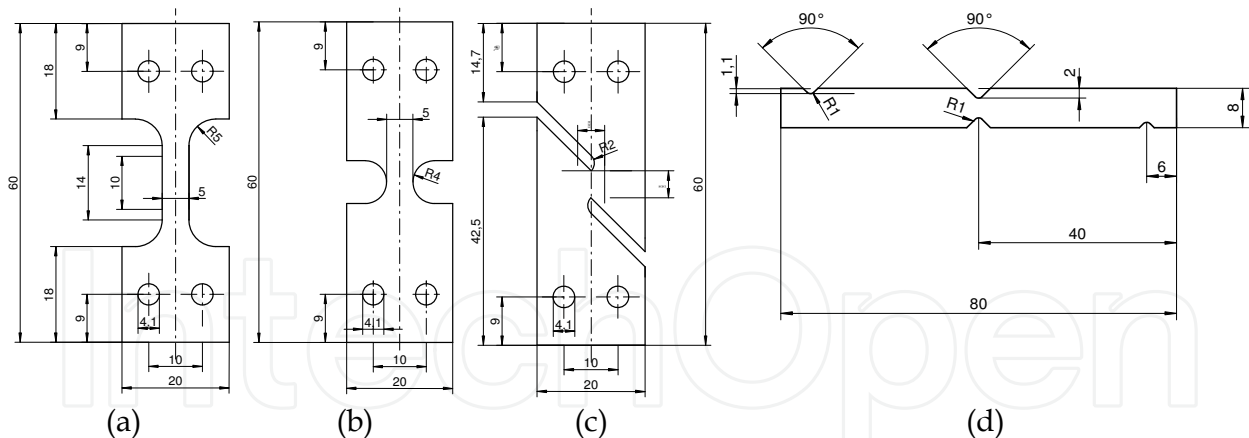Table. 1. Various tests for material modelling

Fig. 1. Sample size for different tensile and shear tests
(a) smooth tensile, (b) notch tensile, (c) double notch tensile, (d) Isoipescu shear
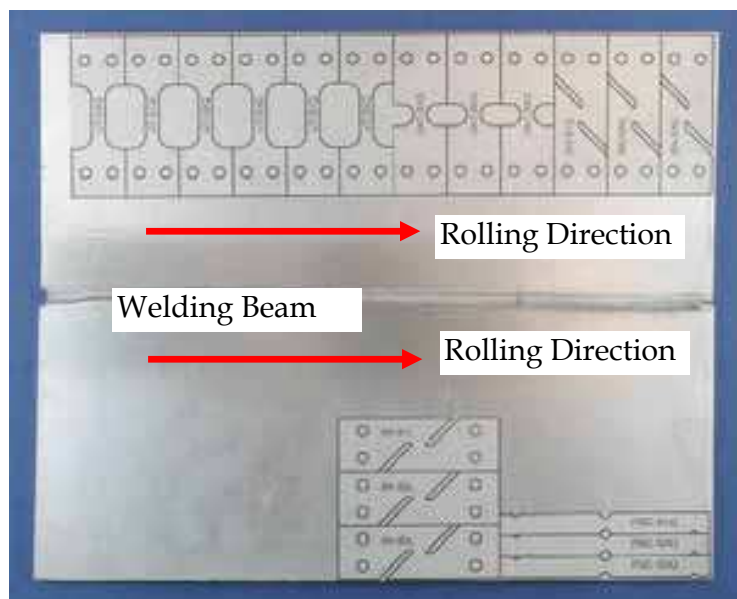

Fig. 2. Distribution of test samples on original plate

Taking PT1-UT-S1Q as an example, the meaning of serial codes can be expressed as followings:

PT1-Project No.; UT-Uniaxial tensile; UNT-Notch tensile; DNT-Double notch tensile; PSC-Isoipescu shear; S1Q-Static transverse sample 1; D2L –Dynamic longitude sample 2

2.1.2 Static uniaxial tensile test

Uniaxial smooth tensile test is one of the basic mechanical tests. The primary aim of this test is to measure the true stress-strain curve and fracture strain. In order to provide with material property for next numerical simulation, so as to expand the scale of the test data, obtain practical data as much as possible; the experiment adopted two sets of equipments. one is the strength-displacement detect system, which uses extend-measurement displacement, also loading sensor to measure load, which is owned by Instron 1886 tensile test machine. Another set of machine is optical deformation measure system, including static camera, digital transition card and following image processing software and diagram

calculation software. The system is equipped with two sets of digital camera; the shooting angle is perpendicular to front side and lateral side of the specimens. Therefore it could detect changes in width and thickness direction immediately when the specimen is in the tensile process, with dynamic image detecting to acquire changes in specimen section, so we could calculate the minimum section size Ai, according to the formulation to calculate the actual stress, strain in tensile process, which could get stress-strain relation of the tensile specimens after necking. In this research two sets of equipments were introduced to work collaboratively. One is normal mechanical test system, another is optical measurement system. The common mechanical testing system is mainly responsible for recording of whole course loading detection and elastic deformation and partial ductile deformation (before maximum loading), while the optical detecting system aim at recording of detection of elastic and ductile(before fracture) deformation.

From Fig. 3, it can be seen that the true strain of aluminium alloy 5052H34 is 0.096 correspond to static maximum tensile load at room temperature, and fracture strain ε_f is 0.73 at this time. These data segment is undetectable by using ordinary tensile experiment, and there will be severe error in the coming up numerical simulation. By contrast, segment data after necking can be repaired if optical detecting system is used, and the maximum true strain can be measured up to 0.561. The measure problem of stress-strain curve can be fixed by linear interpolation. Comparison of Curves of specific materials and precision of numerical simulation will be discussed in this chapter in related diagrams.
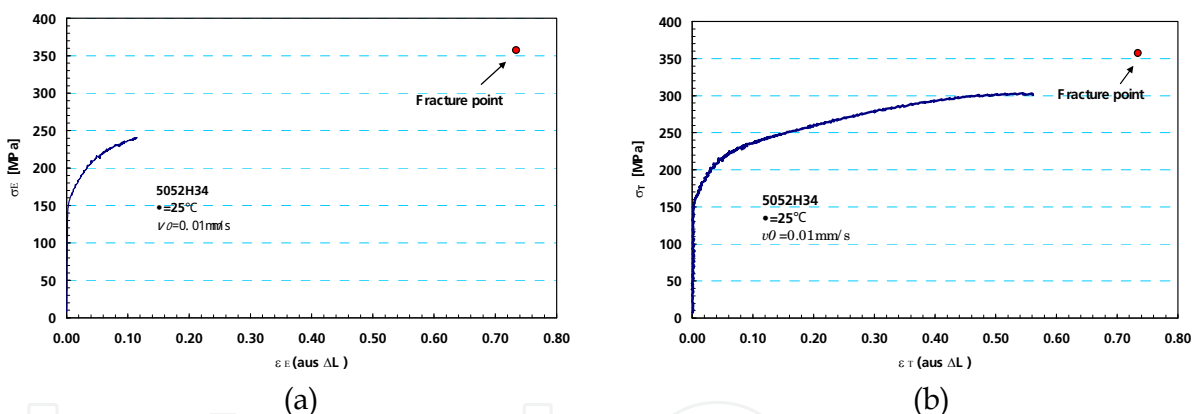

Fig. 3. Comparison of true strain stress curve tested by different devices.
(a) tested by mechanical machine, (b) tested by optical inspection system

2.1.3 Results
1.   Strain and stress curves
The true strain stress curves obtained by two sets of different detecting systems can be shown in Fig.3. The optical deformation testing system is better than the mechanical system for data collection. However the complexity and costs of this optical system is relatively higher.
2.   Material characterization of anisotropic and stress state
Specimen of smooth tensile test is cut from the plate with longitude and transverse direction. The engineering strain stress curves can be seen in Fig.4. Result shows that longitude yield stress is 22Mpa higher than that of transverse. Ultimate strength is 26MPa difference between two directions, which demonstrates particular anisotropic. The size and

distribution of grains is regular from further research in microstructure. First of all, grain size of the surface is larger than centre (Fig.5). Secondly, there is certain grain orientation in the centre of the material because of a rolling process (Fig.6). Grains were extended in the axis along the rolling direction, which caused grain refinement along the thickness direction during rolling process. In the following anneal and artificial aging, there are certain preferred orientation in the refined grains after grain growth or recrystallization, and these factors lead material with certain anisotropic.
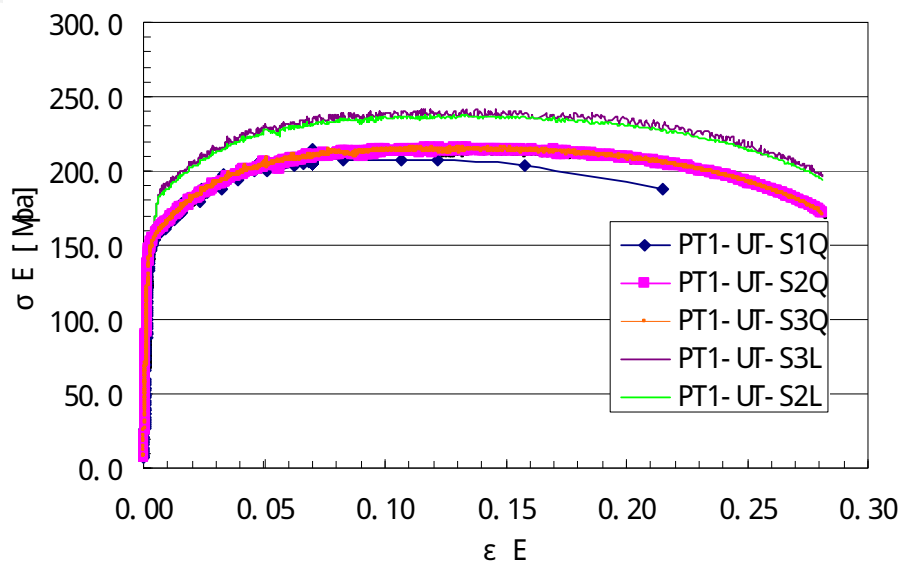
Fig. 4. Strain stress curves for longitude and transverses direction

Fig. 5. Microstructure comparison between surface and centre area
(a) Surface   (b) centre area

Fig.7 compares smooth tensile test with notch tensile test, the notch radius is 4mm, the test showed that the deformation resistance increased at notch condition. With the same deformation, load of smooth test is lower. Triaxiality is bigger at the foot of notch under geometry restraint. In the simple tensile process, larger additional stress derived from the thickness and width direction, and then tri-axis tensile stress formed. Effective shear stress or equivalent Mises stress that ductile deformation needed decreased, which would lead to

ductile difficulty. From the microcosmic aspect, minish the, stress triaxiality of increased with notch radius reducing; stress concentration increased at the foot of the notch, ductility decreased, and fracture strain decreased too. The yield strain of the notch specimen is 4.19%,which is only 35% of the engineering strain of smooth tensile specimen. From the experiment analysis, it's clear that stress condition is not related to yielding obviously, but it matters badly to losing effectiveness of fracture.

Fig. 6. Microstructure of rolling plate 5052H34
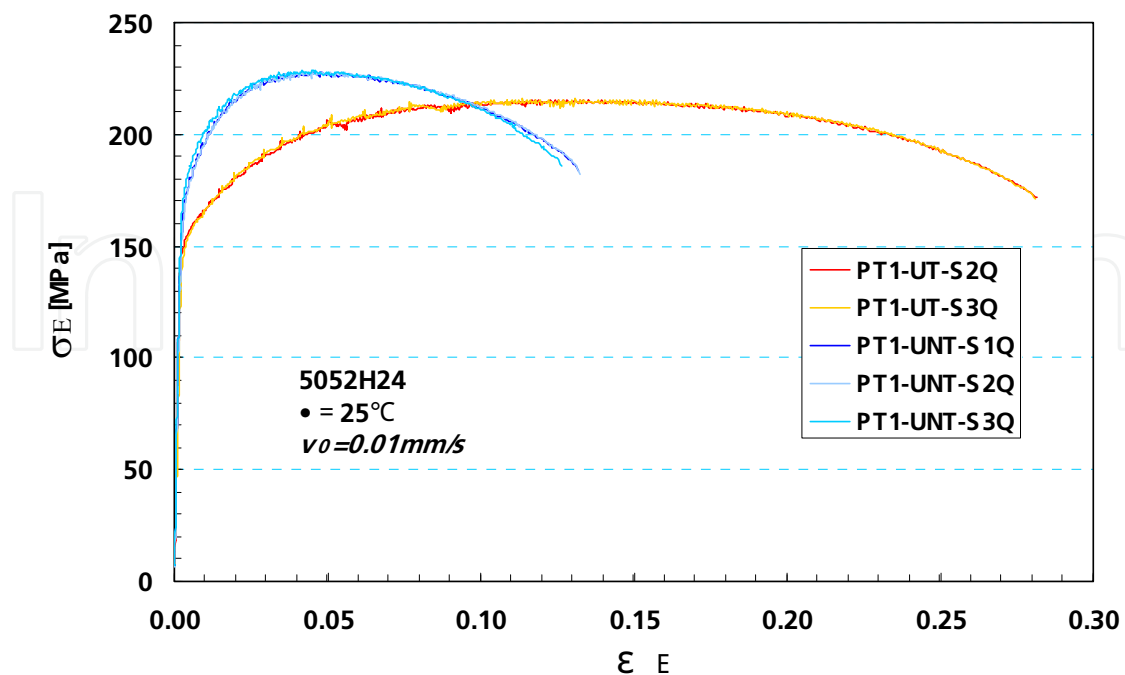
Fig. 7. Strain stress curves of smooth tensile and notch tensile

2.1.4 Dynamic tensile test

1. **Experiment equipment and measurement principle**

   Most of the transportation accidents happened at the velocity of 50Km per hour, the impact kinetic energy of mid-weight car can be up to 150KJ. And the strain rate of these similar impact accidents is about $100s^{-1}$, but the limitation of local strain rate is within 1×10^{-3}. Mostly, the strain of dynamic test is in the scale of $10^2\sim10^3s^{-1}$ on the basis of safe impact design. Currently, the applied test equipments are as follows:

   a.   Falling weight device

   Different heights of falling hammer acquire various kinetic energy, experiment data are collected and processed by using signal processing device. Advantages of such devices are simple structure, easy operation and low costing. It fits impact tests of the level of 10m/s. Previously, there have been such devices such as Qsinghua University; State Key Laboratory of Automotive Safety and Energy and Haribin institute of technology throughout the nation.

   b.   Ejection experiment devices

   There are vertical type and horizontal type, it gains great speed by exploded high energy balloon, the specimens are fastened on data acquisition board with piezoelectric sensor, specimens are impacted with hammer loaded with different masses, while record the impact process with high-speed camera. Advanced digital shooting technology can acquire video image of 10000 frames per second, and the frequency of impact data reach up to 200kHz.At present, all the advance institute are capable of this test, such as Cambridge, Kaiserslautern University and Fraunhofer IWM mechanical institute ,who use this device to test impact responses of components.

   c.   Improved Hopkinson draw(press) poles test devices

   This method is first proposed in 1914, it's the earliest method of testing transient state pulse stress. lately, many researchers changed and developed this method, in which the improved discreet Hopkinson draw poles by Koisky is the most typical one, that has become major testing tool of dynamic property of material. This kind of experiment is taken in metallic large deformation dynamic mechanism response of strain rate within $10^2\sim10^4s^{-1}$.

   The key point of Hopkinson's testing technology is to assure that separate the stress wave effect with dynamic buckling effect within the impact load. Therefore, the incidence pole and test pole of the test device are designed to be longer, in order to separate the influence from reflex waves of press pole, so the equipment would take much space. On the other hand, due to the strict restriction of specimen size, which could make sure ductile stress wave in the component take small proportion in structure buckling response time, compress stress is well distributed in components. Key physical qualities need to be determined in this experiment are as follows:

   Input response of impact load

   Response, value and distribution of structural load

   Response, value and distribution of structural displacement

   Strain rate of material, the key formula are as follows:

   Process of impacting load

   $$P(t) = A_I E \varepsilon_I(t) \tag{1}$$

   Course of input and output loading response of components

$$F_{input}(t) = A_I E \left[\varepsilon_I(t) + \varepsilon_R(t) \right] \tag{2}$$

$$F_{output}(t) = A_0 E \varepsilon_I(t) \tag{3}$$

Course of input and output displacement response of components

$$S_{input}(t) = C_0 \int_0^t [\varepsilon_I(t) - \varepsilon_R(t)] dt \tag{4}$$

$$S_{output}(t) = C_0 \int_0^t \varepsilon_I(t) dt \tag{5}$$

A1 and A0 represent section surface of input pole and output pole superlatively, E represents elastic modulus; $\varepsilon_I(t)$ is course of input strain and $\varepsilon_R(t)$ is the course of response strain.

Since the disadvantages of complexity and bulky of Hopkinson's test device, many researcher have improved it in recent years (Nicholas et al., 1982). One case is to replace impact devices to concussive bullet shoot by high-pressure gas gun, which reduced the size of device greatly and the flexibility increased as well. This innovation made dynamic impacting tests popular.

d.   The improved ejection test device in this research

Considering the effectiveness and convenience of dynamic tensile experiment, making full use of previous equipment, a new particular type of dynamic tensile device-Instron VHS dynamic tensile test machine in Fig.8 was used in this research. Components of such experiment system can be show in Fig.9, including three significant part.

1. Executive part of loading. Pneumatic chuck is the key part, Fig.10 shows the prepare condition of the part before testing, the upper is tied on the fixture, well the below is connected with following system. When the below fixture of testing machine reaches certain speed downside driven by high-energy gas, follow up system would fasten fixed part of the specimen below, which could make the down fixture move along with specimen below synchronously.

2. Zimmer laser-transient displacement high speed photography and force testing part. When lower clip tied up with specimen to move downward synchronously, this would trigger the laser sensor at the same time, and then turn on the high-speed camera, which would record deformation and displacement of the specimen with the scale distance. Sampling frequency of shooting is 2500fps. Analyze relationship between displacement and time of scale boundary by means of later digital image processing. Comparison of calculation error and data of local foil gauge is smaller than 5%.Measurement of tensile load via acceleration sensor to multiply instantaneous acceleration by quality to get changes of system dynamic load. Formula 3.6 shows the calculation in details

$$P(t) = M[g + a(t)] \tag{6}$$

Where P (t) is instantaneous tensile load represents movable chuck component is acceleration, a (t) is instantaneous acceleration. Accordingly, whole deformation energy and impact energy can be derived by integral calculus of compounded load-displacement.

3. Data collection system. It includes digital oscillograph, later treatment part of computer. Digitalize the amplified signal, with filtering waves; lastly, digital documents will be stored in computer. The filtering process adopted high-frequency filtering circuit and spine fit smoothing technique of ultimate data. The advantages is that sorting of wave characteristics can be artificially controlled, in accordance with various experiment condition to choose filter function, which can avoid data distortion inn filtering by means of adjusting smoothness. Common spline function is demonstrated in formula 7

$$f_t^{'} = \frac{1}{32}(5f_{i-1} + 22f_i + 5f_{i+1}) \tag{7}$$

f_{i-1}, f_i, f_{i+1}, represent function value of i-1, i and i+1. f'_t represent the function value after t times filtering, this function can be iterated endlessly till the result is satisfied.
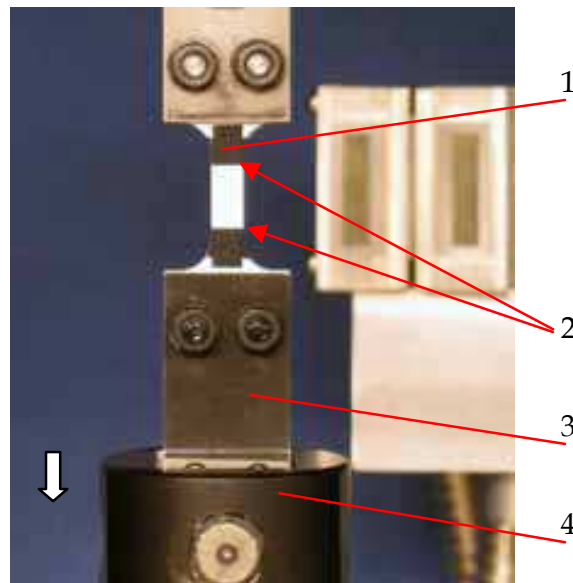
Fig. 8. Dynamic tensile test
1 sample, 2 fixture boundary, 3 fixture, 4 cross head

e.   Size of specimen and initial conditions
Specimen size is as same as the static tensile one; orientation of specimens is perpendicular to rolling directions. Install foil gauges symmetrically on two sides of the specimen within the measure scale before experiment, so as to adjust twist error in dynamic tensile test. Meanwhile print glisten glue of light colour in the centre of test zone, which is used to high-speed photography. Finally fix the whole specimen in the tensile fixture, and adjust laser trigger.

2.   **Experiment result**
Relationship among engineering strain, initial tensile velocity and scale distance in dynamic tensile test can be demonstrated as

$$\dot{\varepsilon}_{nom} = \frac{v_0}{L_c} \tag{8}$$

In this experiment, it's certain that initial velocity of fixture v_0 is 1.7m/s, scale distance is 10.08mm. Average strain rate is 169s-1, according to formula 8 at tensile condition. Fig. 9 shows the curve of load-displacement at dynamic tensile condition. Fig. 10 demonstrates the relationship among engineer-stress, strain and true stress-strain.Fig.11 shows the comparison between dynamic load and static true stress.
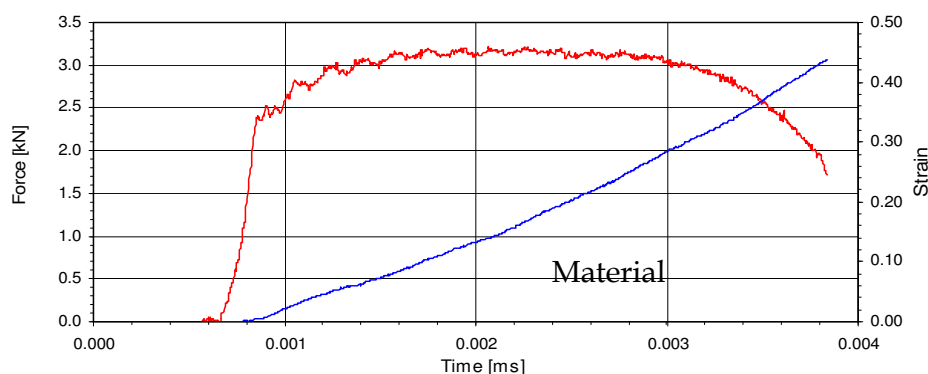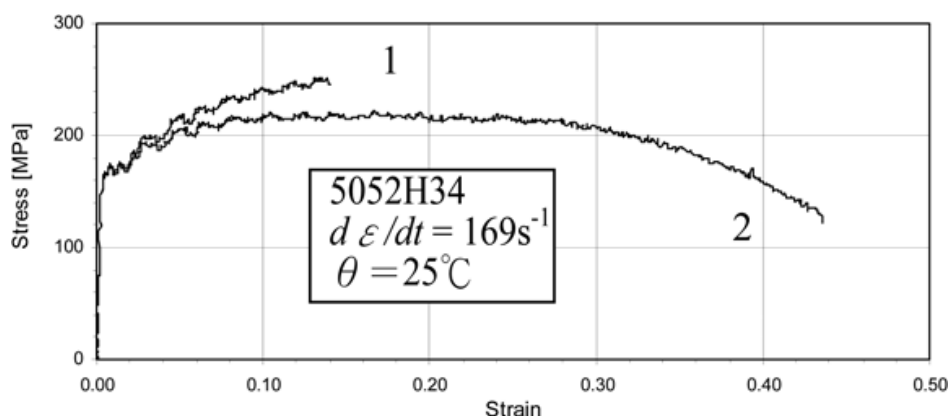

Fig. 9. Load and displacement curve

Fig. 10. 5052H34 strain stress curves
1 true strain and stress, 2 engineering strain and stress

Fig.12 is the comparison of engineer stress-strain measured by static notch tensile, smooth tensile and dynamic load smooth tensile test.Fig.13 shows that static and dynamic strength of material and plasticity index vary with strain rate. The data imply the slight improvement of the aluminium alloy strength with the strain rate increase from dynamic to static tensile, by contrast, the fracture strain increase by 60%, shrinkage of section increase by 18%, which means the ductility is enhanced. High-speed deformation is done in short time in dynamic loading test, a lot of heat is generated and unable to consume, so it could be treat as a non-exchange heat process with the outside. So temperature of local material would rise dramatically, mechanism response of material has become a heat-stress coupling problem. On the basis of document, as for Al-Mg-Si alloys, work hardening and dynamic softening are concurrence under condition of large strain rate, they are paradoxical on the affection of mechanism property. In the process of elastic deformation, crossing, propagation and accumulation of dislocation lead to networks of dislocation, which caused work hardening, the higher the strain rate is, the larger resistance of slip movement of dislocation will be.
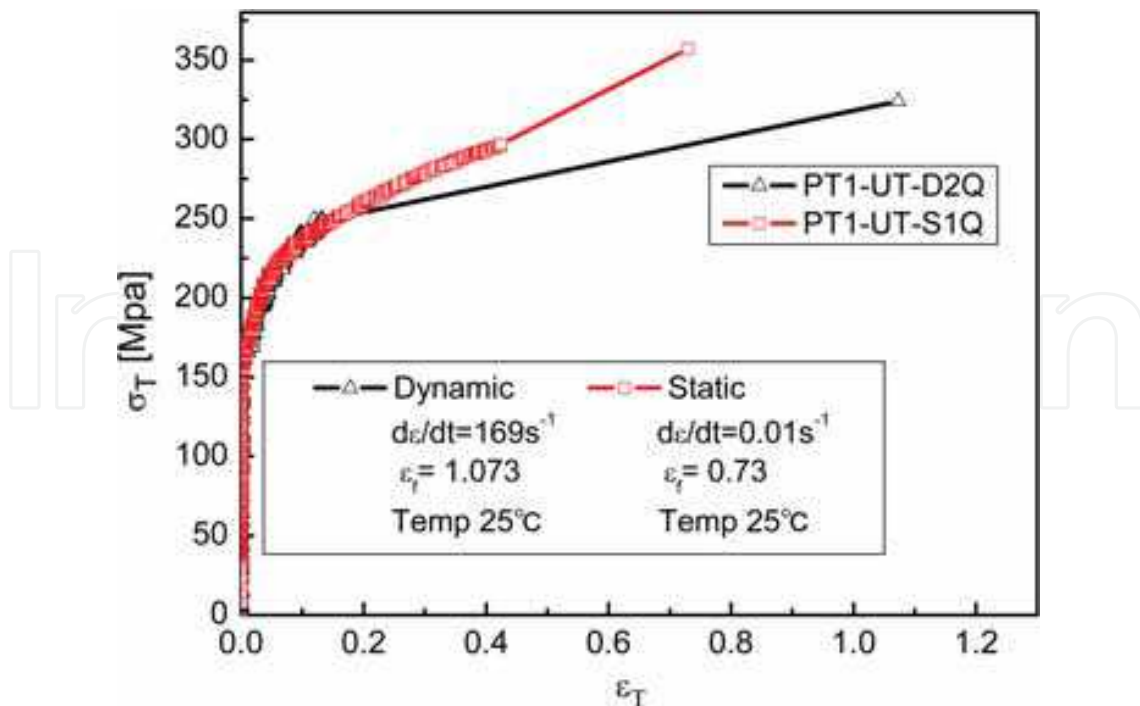
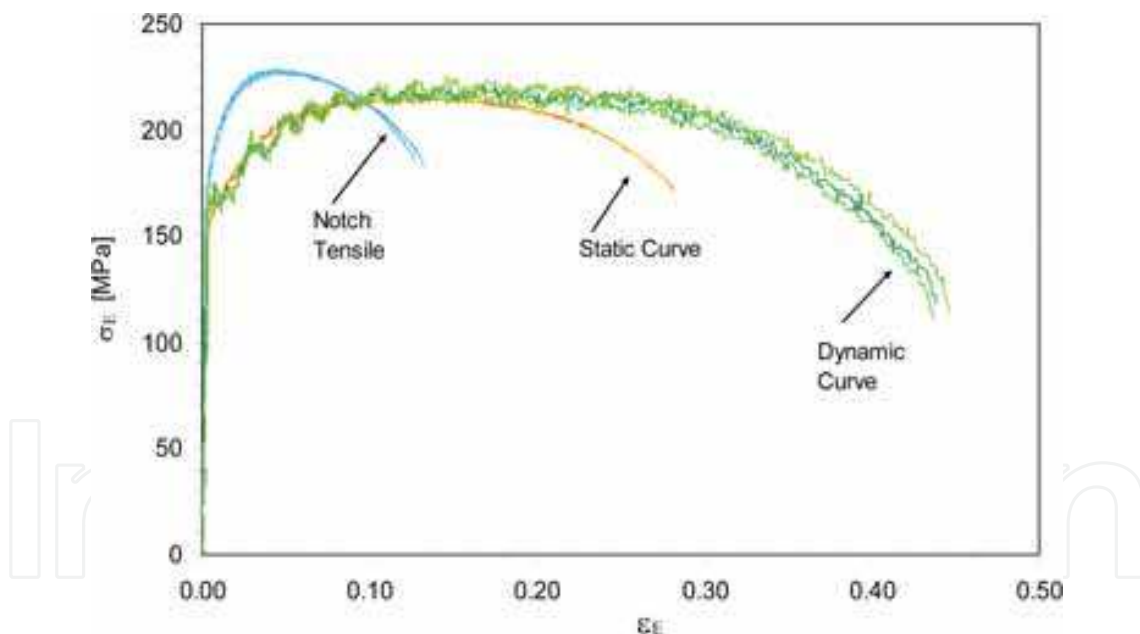Fig. 11. Dynamic and static true stress and strain curves

Fig. 12. Effects of stress state and strain rate on material flow property

Material deforms in the way of twin crystal, yield stress and flow stress grows with the increase of strain rate. But, as for aluminium alloys, R.Mignogna.etc found that the strain rate sensitivity is lower at temperature index is smaller than 0.1, so yield stress would improve slightly with the increase of strain rate. Comparing with the 6063 aluminium alloy, data of stress-strain rate hit off with our result (Fig.13).With the temperature increasing, strain sensitivity grows significantly. When the temperature surpasses half of the melting point, m values between 0.1 and 0.2.

All in all, notch sensitivity of aluminium alloy 5052H34 is strong. With stress triaxiality grows, the plasticity decrease. However, dynamic and static tensile test prove that material strength at room temperature is not sensitive with strain rate, but sensitively grow with increasing of ductile strain rate, which has close association with dynamic softening in thermal isolation process. We need to fully consider affection of temperature to plastic flow in constitutive model of material. Temperature's influence on flow stress will be discussed in detail in up coming chapters.
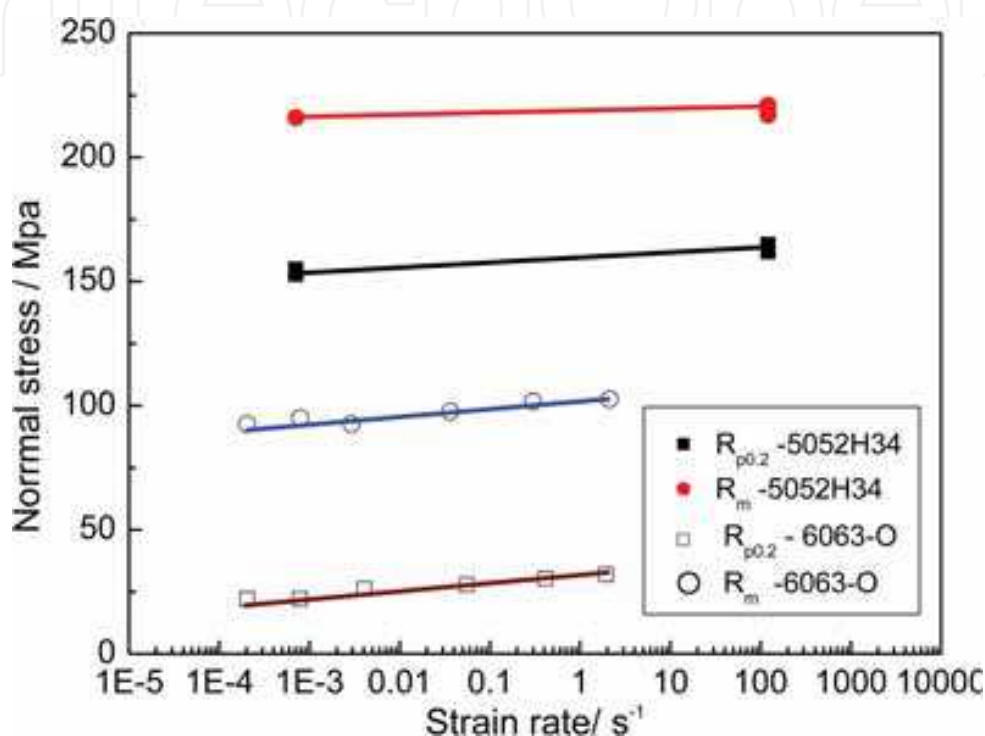
Fig. 13. Relationship between strength and strain rate

2.2 Shear test
2.2.1 Introduction of shear test.
Shear damage is one of the most common failure in car crashes. Especially, the thin-walled components such as buffing tubes and frameworks, etc. Shearing, buckling and tearing always happen in crashes. So, how to use simple and effective method to research shear deformation and failure detail, acquire characterization of key materials that really matter to whole characterization and model-building.

Previously, shear test such as twisting, quasi-static punching and Iosipescu shear test have been widely accomplished throughout the world. Precision and effectiveness of these tests have been confirmed by numerous application, but it still proved its limitations. Generally, Iosipescu and twisting tests are used in static experiments, and can hardly expand to dynamic shear research of high strain rate. In this case, we are trying to design a kind of new double notch shear test and method, which could be adopted in static and dynamic shear validation. So as to confirm effect of this new type of shear test, we used Iosipescu test as a reference to analyze the advantages and disadvantages of this double notch test.

2.2.2 Specimen size and experiment equipment

1. **Double notch shear test**

In this experiment, we designed a kind of tensile specimen to test failure process and shear damage of plate materials.Fig.14 shows the appearance and sizes of specimen. Notching at two parallel sides of the specimen, notch angle with the neutral axis is 45 degree. The design of other geometry parameters is identical with normal tensile specimen. Fix the specimen on tensile test machine during experiment, the minimum available section is the plane between two notch tips, where would occur yielding very first at tensile process, and then shear deformation develop in the direction of tensile axis till facture.

In order to observe the deformation between two notches during tensile process, draw the grid lines on main deformation zone before experiment. Record the process of deformation by digital shooting system, while output the data of load and displacement within scale distance. Fig.15 (a) shows the control panel of the experiment and (b) shows test device.

(a)   (b)
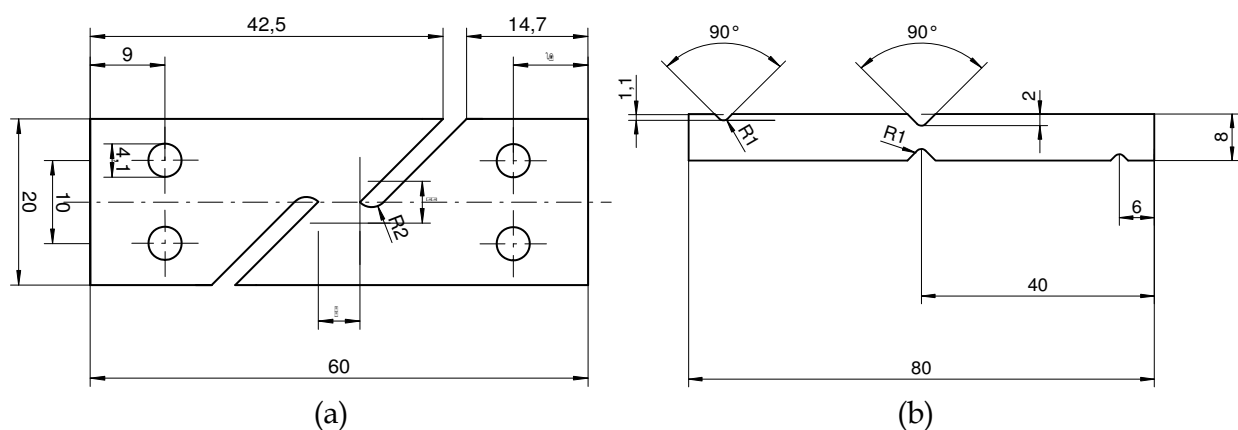
Fig. 14. Sample sizes for shearing test
(a) Double notch tensile test, (b) Iosipescu shearing test
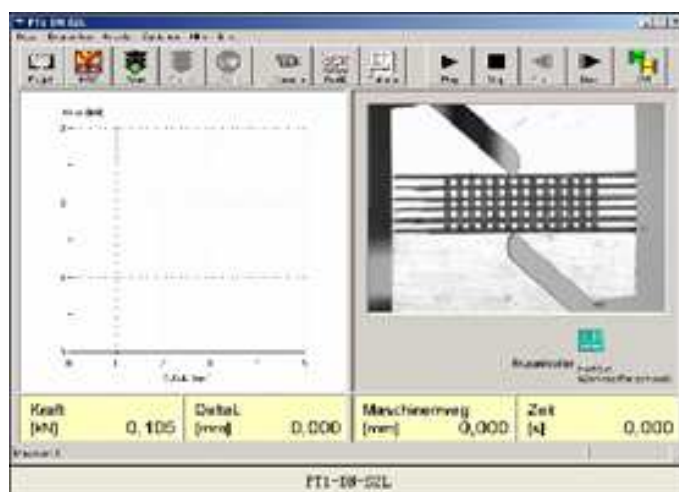
(a)   (b)

Fig. 15. Shearing test devices
(a) Interface of monitoring system for double notch tensile test
(b) Equipments for shearing test

2. **Iosipescu shear experiment**

Fig.14 (b) shows the specimen size,Fig.15(b) is the experiment device. The specimen is fixed on test machine with four rigid cylinders. With up chuck pushing downward, specimen would be damaged and shear deformed. According to force analysis, theoretically, shear place should locate on the vertical surface of the specimen's central symmetrical axis. Local deformation can be measured by strain gauge, meanwhile record the process by digital photography.

Under static condition, the loading rate of double notch test and Iosipecu test is 0.001m/s.Type of testing machine: Instron material tensile testing machine.
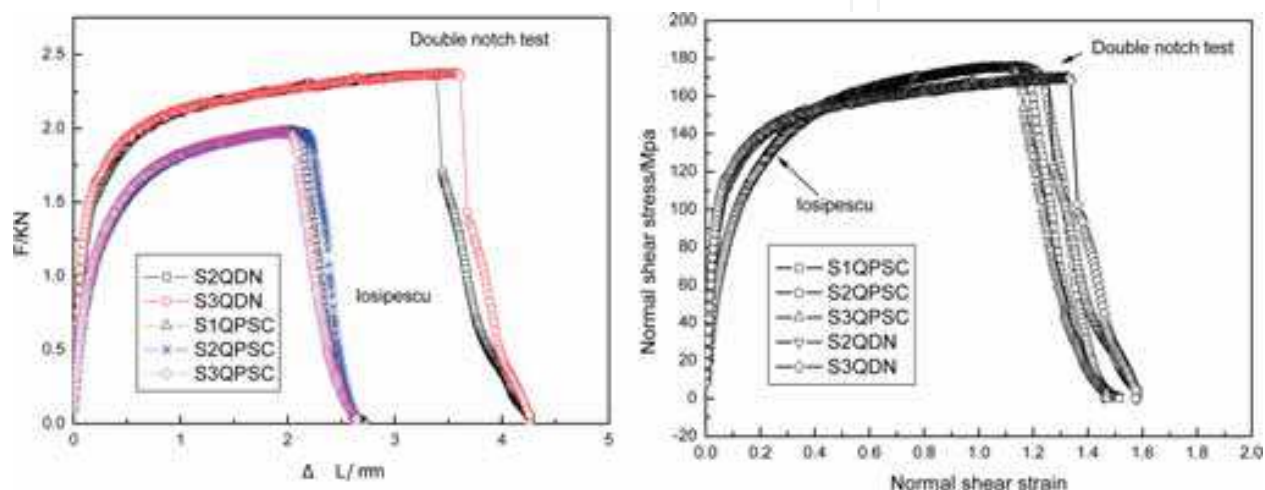
Fig. 16. Displacement and load curves for double notch tensile and Iosipescu shearing test

(a)	(b)
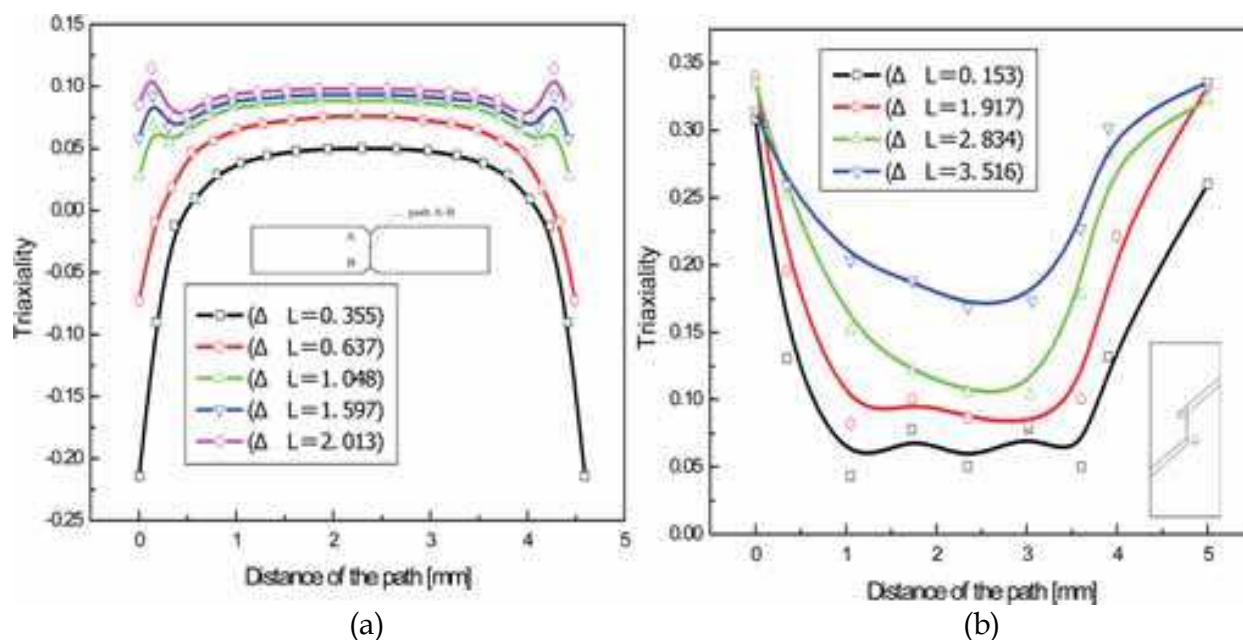
Fig. 17. Comparison of triaxiality for Iosipescu and double notch tensile
(a) Iosipescu shearing test, (b) double notch tensile test

3.   **Test results**

The displacement and load curves of shear tests are shown in Fig. 16. When deformation is small than 0.5, the strain stress curve of double notch tensile test is higher than Iosipescu; when the deformation is larger than 0.5, the curve of Iosipescu exceeded that of double notch tensile. The maxim stress of double notch tensile test is 169.8MPa as well as 175.6MPa of Iosipescu. The difference is 3.3%. The fracture strain is 1.28 for double notch tensile and 1.6 for Iosipescu. The difference is 9.3%. In a general view, the results of two experiments have good agreement with each other, which means the double notch tensile test is comparable for a standard shearing test.

Fig.17 shows the evolution of triaxiality during deformation for double notch tensile test and Iosipescu shearing test. It can be seen from the results that average value of triaxiality about DNT (double notch tensile) is from 0.1 to 0.3, mean while, the triaxiality changed from 0.05 to 0.15 for Iosipescu shearing test.

Fig. 18 shows the distribution of stress state and concentration for the two kinds of tests.
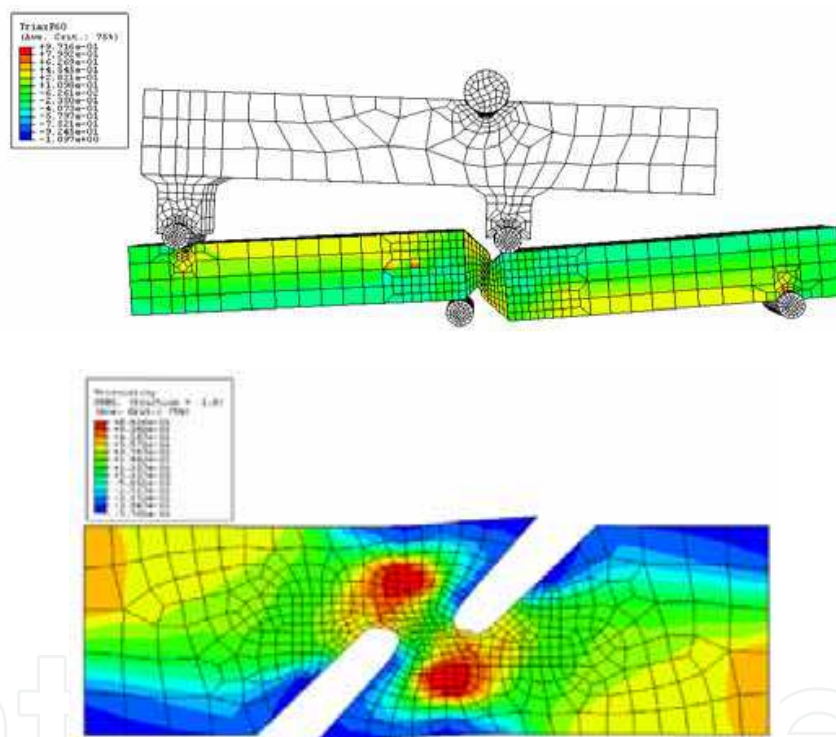
Fig. 18. The distribution of triaxiality for Iosipescu and double notch tensile test

3. Inhomogeneous deformation and damage modelling for aluminium alloy welded joints

3.1 Experiment procedure

The small punch test (SPT) has been used by numerous researchers to test mechanical properties of various materials, especially for steel, copper, magnesium and aluminium. The test programme and experimental setup are described in great detail in related reference (Asif et al., 2004). Based on the general idea of SPT, a small punch-shearing test setup was established for this study. In brief, it consists of a thin sheet specimen with the thickness of 2mm, specimen holder, shear punch, punch die, and fixture.

There are two types of specimens used in this study. One is made of homogeneous materials, such as Al alloy 6063. The other is made of inhomogeneous materials such as a sheet butt joints welded by TIG. The specimens were shaped 24mm×50mm rectangular pieces. The surfaces of the specimen are mechanically polished by emery paper (grain size 320) to obtain the desired thickness (i.e. 2 mm thick) in each case. Fig.19 shows the schematic diagram for the small punch test experimental setup.

A special rigid punch of 1.5 mm diameter with a flat tip was designed for small punch test. The offset of the diameter is less than ±0.03mm. In order to concentrate the punch plastic deformation below the punch area, a small clearance between punch and dies was left during punch test. The clearance was identified by equation 1.

$$z = mt \tag{9}$$

Where z is the maximum clearance between punch and dies, m is correlative coefficient. For aluminium alloy m, it is equal to 0.06, and t is thickness of the specimen. For example, for the aluminium alloy 6063 sheet specimen, if the thickness is 2mm, Z is 0.12mm. Therefore, considering the accuracy of punch, geometrical dimension of the punch die would be less than 1.77mm.

Specimen holders and lower dies were included in a homocentric structure, which keeps the upper holder precisely fitting the lower die. Rectangularly shaped specimen was placed into the lower die, and was fixed by four screw bolts. Miniature specimens are carried out at room temperature and static condition using an instron testing machine. The loading speed of punch was 0.5mm/min. For each case, at least three punch specimens were tested to ensure the stability of results.
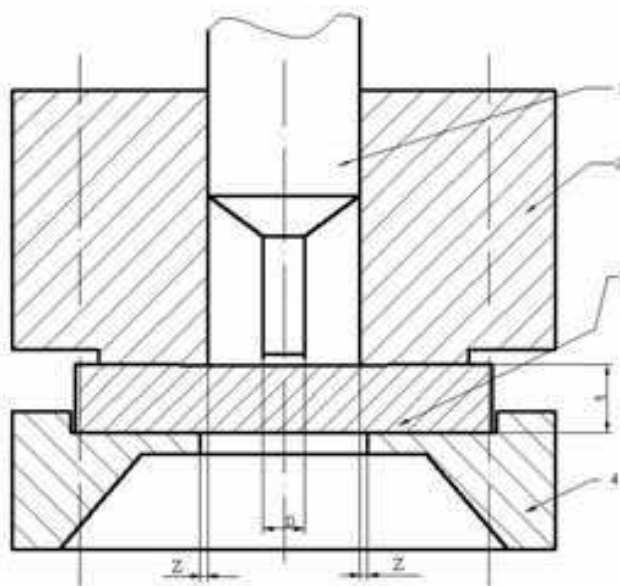

Fig. 19. Experimental setup of the STP
1. punch, 2. holder, 3. sheet specimen, 4. die

Three types of homogenous materials: copper; Al alloy 5052; and Al alloy 6063 T5 were tested by the small punch test setup. Their displacement vs. punch force curves are shown in Fig. 20. During the punch process, the specimen had experienced three specific deformation stages. First, elastic deformation, then plastic deformation and finally a
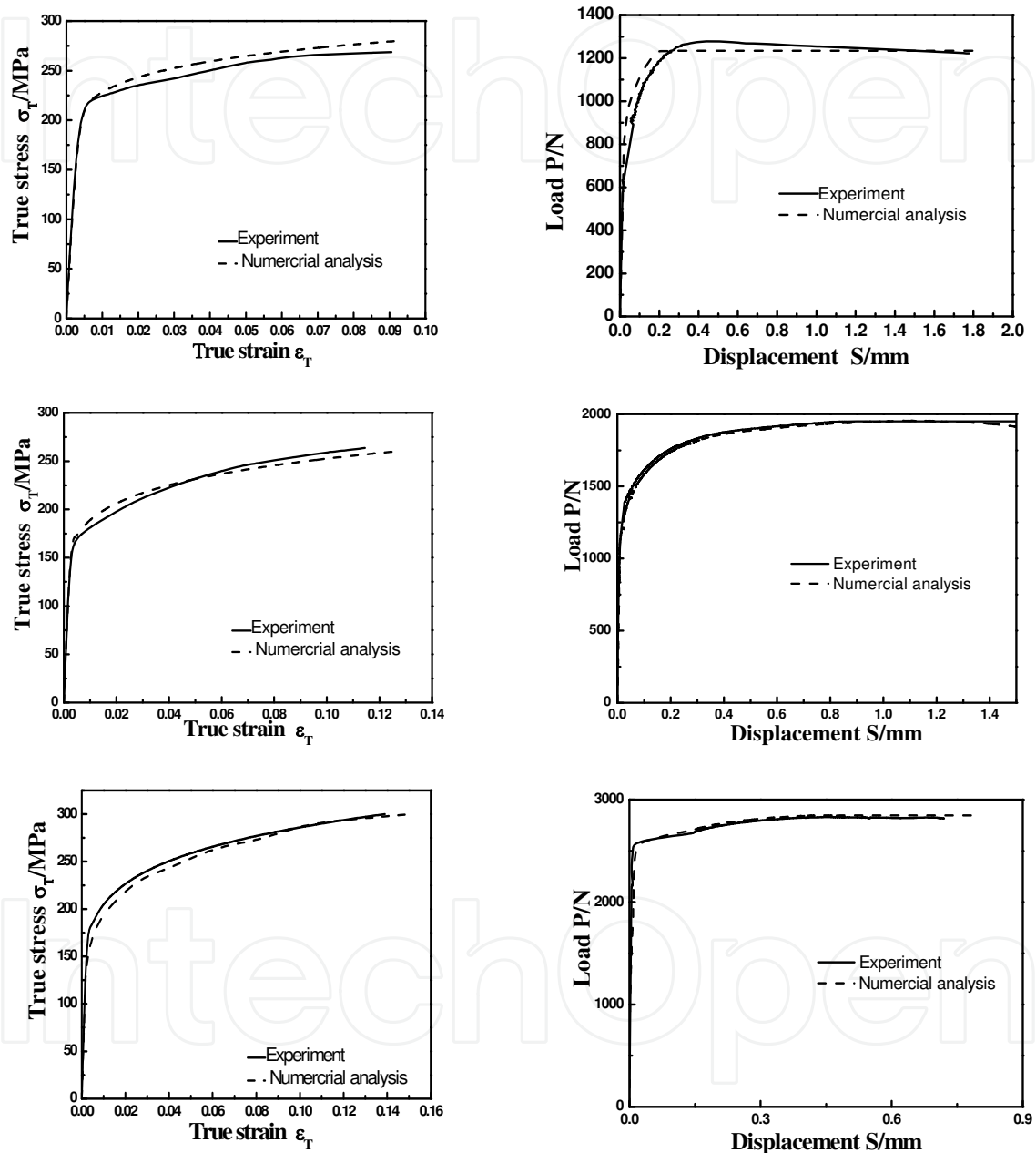
Fig. 20. True strain-stress and load-displacement curves of SPT

fracture. The specimen surface was subjected to a composition of shear force, friction force, and pure pressure.

3.2 Inverse finite element procedure

For this study, the inverse FE procedure was tried to identify the true strain stress curve of unknown materials. The experimental load-displacement curve is used as an input in linear, step by step, iterative process of FEM for comparison. The outputs of this inverse procedure are: the modulus of elasticity of the unknown material; true stress vs. true plastic strain curve, starting from yield stress and corresponding zero plastic strain. The pictorial algorithm is shown in Fig. 21 and the iterative process is expressed as follows:
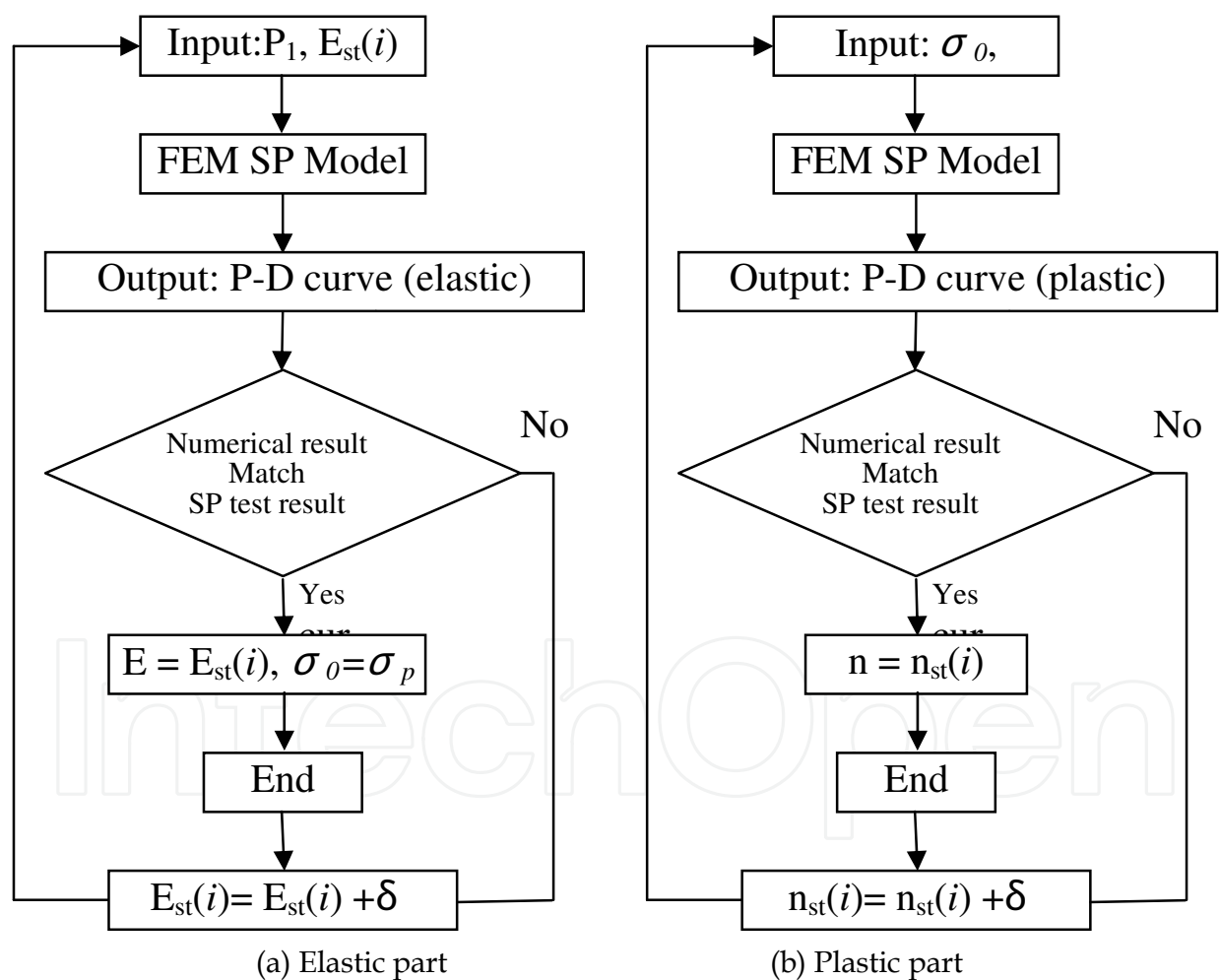
Fig. 21. Diagram of inversed FE procedure from SPT

1. the small punch experimental load *vs.* displacement curve is divided into two parts. One is the elastic linear segment. The other part is nor linear elastic-plastic segment, which can be expressed by the exponent function of Eq. (2).

2. for the iterative process of the elastic segment, the inputs are punch load P1 (elastic peak load) and an assumed starting value of modulus of elasticity E_{st}. The outputs are punch load *vs.* displacement curve which try to match the actual experimental load-displacement curve by increasing or decreasing E_{st} during each iteration step (value of δ). The final value of E_{st} should be equal to modulus of elasticity E of the material and maximum equivalent von-Mises stress of the specimen equal to the yield stress of the material.

3. for the iterative process of the elastic-plastic segment, the true stress and strain can be expressed as equation (10).

$$\sigma = \frac{\sigma_0}{\varepsilon_0^n}\varepsilon^n \qquad (10)$$

Where the σ, ε are true stress and strain; σ_0, ε0 are yield stress and yield strain, which has been from the previous step (2); *n* is the hard coefficient. During this nonlinear segment, the inputs are σ_0, experimental maxim punch load P_k and assumed hard coefficient n_{st}. The outputs are punch load *vs.* displacement curve which was matched to that of experimental data by changing the value of n_{st} the final value of n_{st} would be equal to the hard coefficient *n* of the material.

4. after the iterative calculation, the mechanical property of the unknown material can be described by material parameters of elasticity modulus E, yield stress and strain σ_0, ε0, and hard coefficient *n*.

3.3 Validation of material modeling and discussion
3.3.1 Mechanical behavior determination for homogeneous materials

Fig. 20 shows the comparison between true stress-strain curves obtained from the uniaxial tensile test and those of predicted results using inverse FE arithmetic for SPT specimens of three different materials. The results show that numerical models agree well with the experiment data.

3.3.2 Case of material modeling for butt welded joint

In a welded joint, the microstructure, grain size and mechanical properties are quite different in each specific zone such as HAZ, weld, and base metal. Considering the mechanical heterogeneity the butt joint was divided into ten micro-portions from base metal to welded metal (see Fig. 22) according to the hardness distribution as showed in Fig. 23. Accurate mechanical tension behavior of each micro-portion was obtained by the inverse finite element procedure (Fig. 24). Finally a uniaxial tension numerical model was set up according to the experimental condition. Material properties obtained from the inverse FE procedure were assigned to the specific micro zones. General tensile mechanical behavior was calculated by the ABAQUS finite element code. The simulated and experimental strain-stress curves are presented in Fig.25. The simulation results are in good agreement with thoses of experiments, which means that the mechanical properties obtained from the sp test and inverse FE procedure are believable.
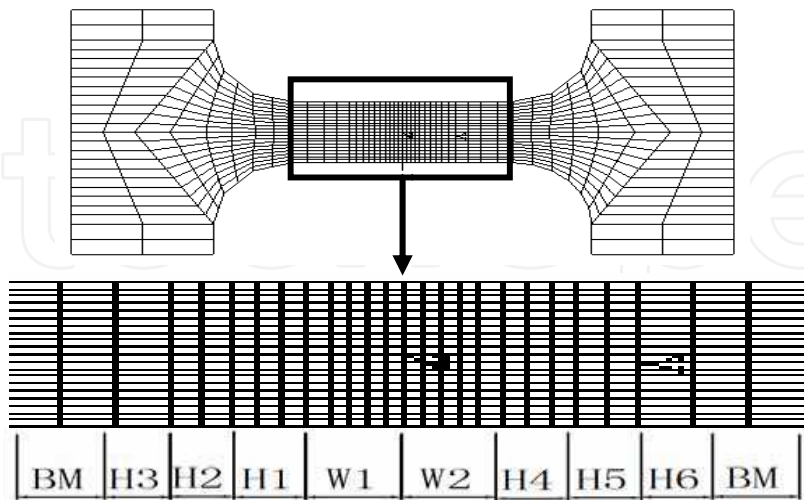
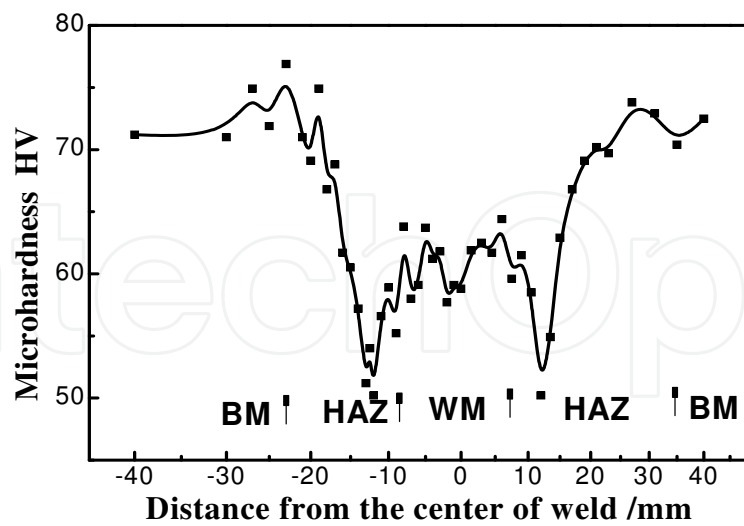Fig. 22. Micro-portions distribution of butt joint

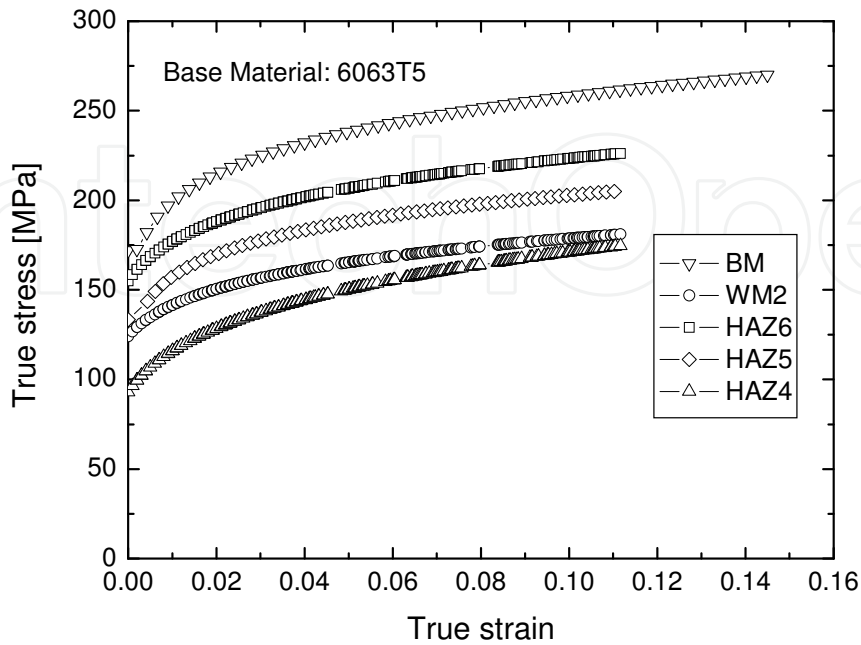Fig. 23. Hardness distribution of butt joint (6063T5)

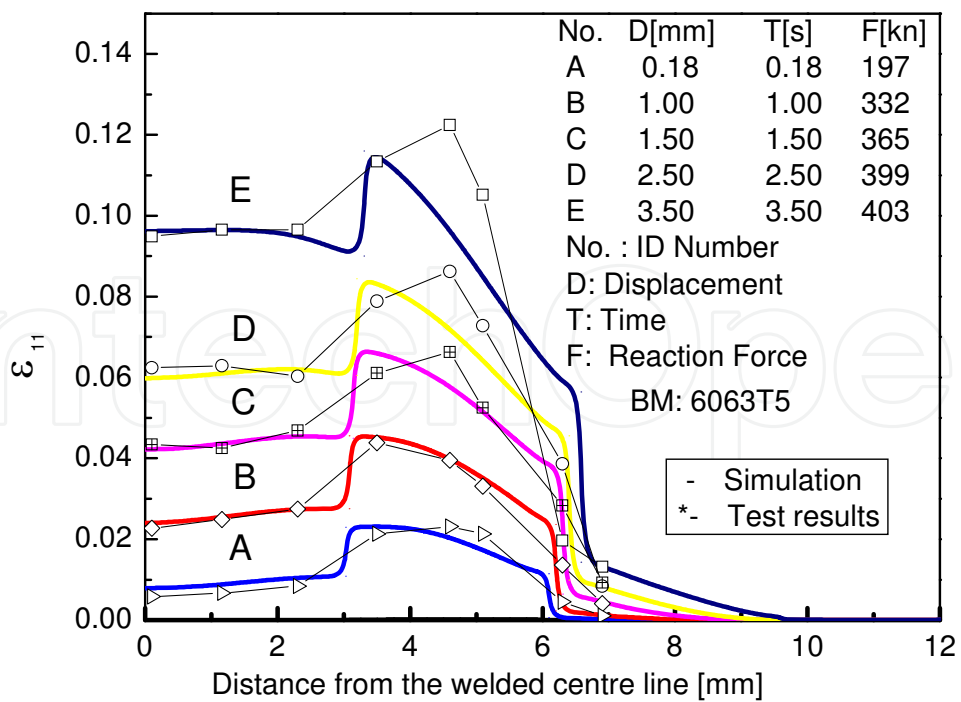Fig. 24. Uniaxial tensile behavior of different micro zones of joint (6063T5)

Fig. 25. Evaluation of Inhomogeneous deformation of a welded joint

4. Conclusions

In the current work, aimed at aluminium alloy 5052H34 and 6063T6, material characterization and modelling have been carried out. Material plastic deformation and damage initialization and evolution were studied under static and dynamic loading with different stress state and strain rate.

In addition that, a new experiment double notch tensile was expressed with related evaluating standard and sample size as well. The test precision was discussed with Iosipescu shearing test by using experimental and numerical data. Results show that the double notch tensile test is a suitable measurement for mater mechanical behaviour driven by shear stress. It can be used not only for static loading but also for dynamic impacting. Combined with Iosipescu shear test, uniaxial tensile and notch tensile test, strain stress relationship and damage parameters were obtained for the two kinds of aluminium alloy.

For the inhomogeneous deformation and damage of welded joints, an inverse FE algorithm based on a SPT experiment was represented for determination of constitutive behaviour of an unknown material. A numerical simulation of SPT to identify the accurate material parameters was carried out. The inverse FE procedure was tested and validated on a case of a butt joint of aluminium alloy 6063T5. The welded joint was divided into ten micro zones along the tension axis. Localized mechanical properties were assigned to the specific sections of joint. Finally the global mechanical behaviour of welded joint was simulated by a numerical model. The numerical tensile load-displacement curve agrees well with the experimental results.

5. Acknowledgments

6. References

Asif Husain, Sehgal D K, Pandey R K. An inverse finite element procedure for the determination of constitutive tensile behavior of materials using miniature specimen, Computational Material Science, 2004 (31): 84-92

Blauel J.G, Sommer. Crashtests and numerical simulation of welded aluminium component with defects. In: 3rd international symposium " Passive safety of rail vehicles" . Berlin, 2002 , 57 - 61

Campitelli E, Spa¨tig P, Hoffelner W. Assessment of the constitutive properties from small ball punch test: experiment and modeling, Journal of Nuclear Materials, 2004 (335) : 366-378

Sun D-Z, Silk Sommer. Characterization and modeling of material damage under crash loading. In: 21st CAD-FEM Users'Meeting. Berlin,2003,98-103

Franck Lauro, Bruno Bennani. Identification of the damage parameters for anisotropic materials by inverse technique: application to an aluminium.Journal of Materials Processing Technology.2001,118(3):472-477

Ghoo B Y, Keum Y. Evaluation of the mechanical properties of welded metal in tailored steel sheet welded by co2 laser, Journal of Materials Processing Technology, 2001 (113) : 692-698

Hankin G, Toloczko M B, Hamilton M L, et al. Validation of the shear punch-tensile correlation technique using irradiated materials, Journal of Nuclear Materials, 1998 (258) : 1651-1656

Johann Georg Blauel, Wolfgang Bosshme. Material characterization for crash simulation. In: CrashMat 2002.2. Berlin,2002,46-50

Nicholas T. Material behavior at high strain rates. Impact Dynamics. New York : John Wiley & Sons, 1982

Zhu Liang, Chen Jianhong. The stress distributions and strength of the welded joints with mechanical heterogeneity. Proceedings of the International Conference on Heterogeneous Materials Mechanics, China Chongqing, 2004:18-24

Aluminium Alloys, Theory and Applications

Edited by Prof. Tibor Kvackaj

The present book enhances in detail the scope and objective of various developmental activities of the aluminium alloys. A lot of research on aluminium alloys has been performed. Currently, the research efforts are connected to the relatively new methods and processes. We hope that people new to the aluminium alloys investigation will find this book to be of assistance for the industry and university fields enabling them to keep up-to-date with the latest developments in aluminium alloys research.

How to reference

In order to correctly reference this scholarly work, feel free to copy and paste the following:

Jisen Qiao and Wenyan Wang (2011). Inhomogeneous Material Modeling and Characterization for Aluminium Alloys and Welded Joints, Aluminium Alloys, Theory and Applications, Prof. Tibor Kvackaj (Ed.), ISBN: 978-953-307-244-9, InTech, Available from: http://www.intechopen.com/books/aluminium-alloys-theory-and-applications/inhomogeneous-material-modeling-and-characterization-for-aluminium-alloys-and-welded-joints

INTECH
open science | open minds